PAPER

ROYAL SOCIETY OF CHEMISTRY

N-Aryl substituents have an influence on the photophysics of tetraaryl-pyrrolo[3,2-*b*]pyrroles

Wojciech D. Petrykowski, [a] Marzena Banasiewicz, [b] Olaf Morawski, [b] Zbigniew Kałuża, [a] Cristina A. Barboza [*b] and Daniel T. Gryko [*a]

The photophysics of two series of 1,4-dihydro-tetraaryl-pyrrolo[3,2-*b*]pyrroles possessing *N*-aryl substituents with various electronic characteristics was investigated systematically. The molecular structure of these compounds was designed so that their solubility enabled us to study their absorption and emission in a broad range of solvents. The presence of *N*-4-nitrophenyl substituents is responsible for a weak charge-transfer absorption band and shifts the emission band hypsochromically. At the same time, their presence quenches fluorescence; although if electron-withdrawing substituents are present at positions 2 and 5, this effect is reduced by an order of magnitude. In the case of less electron-withdrawing *N*-4-cyanophenyl and *N*-3-cyanophenyl groups, strong emission is present only if the electron-withdrawing groups are located at positions 2 and 5. The combined experimental and computational study points out the existence of a barrier between a_u (bright) and a_g (dark) CT states, the height of which is the key factor governing the fate of these molecules in the excited state. Weaker electronic communication at positions 1 and 4 of the DHPP core is responsible for strong charge separation. Polar solvents favor the formation of transient dipole moments due to excited-state symmetry-breaking, which amplifies the nonradiative deactivation of nitro-TAPPs. A large increase in fluorescence intensity at 77 K suggests that internal conversion is a key channel for non-radiative electronic relaxation. Conversely, moderate to weak electron-donating groups favor strong LE emission.

Introduction

The potential of 1,4-dihydropyrrolo[3,2-*b*]pyrroles (DHPPs), originally discovered by Hemetsberger and Knittel in 1972,[1] was negatively impacted by their poor synthetic accessibility. This situation abruptly changed in 2012, when tetraaryl-pyrrolo[3,2-*b*]pyrroles (TAPPs) became easily available.[2] Given the broad scope of substrates tolerated by the discovered multicomponent reaction,[3] the TAPPs became a favorite building block to assemble N-doped non-planar nanographenes,[4,5] and to study excited-state symmetry breaking (ES-SB),[6,7] as well as the perplexing fluorescence of nitroaromatics.[8,9] These studies predominantly focused on the impact of substitution at the carbon atoms of centrosymmetric TAPPs, due to their acceptor–donor–acceptor (A–D–A) configuration, which promotes the population of charge-separated states. These are crucial for applications in organic electronics.[9–12] Numerous studies have explored the photophysics of TAPPs and their π-expanded analogs through both experimental and theoretical approaches.[8–17]

Despite their ground-state quadrupolar nature, DHPPs are susceptible to ES-SB, inducing transient dipole moments that explain the solvatochromism experimentally observed in the absorption spectra.[13,14] The photophysical versatility of DHPP derivatives is further evidenced by their ability to form charge-transfer states sensitive to solvent polarity. This effect is observed when the chromophore is bonded to polycyclic heteroaromatic molecules forming double helical systems, even in the absence of strong donor or acceptor groups bonded to the main dye.[15]

Interestingly, the presence of $4\text{-NO}_2\text{C}_6\text{H}_4$ at positions 2 and 5 highlights how the interplay between intersystem crossing (ISC) and IC affects the fluorescence efficiency of bis-nitro-DHPPs. These molecules show exceptionally large fluorescence quantum yields in non-polar solvents due to slow ISC and weak electronic coupling between nitrophenyl substituents and the main chromophore.[8] Analogous studies reveal that these systems exhibit complex deactivation dynamics, governed by D–A electronic coupling, intra/intermolecular interactions, solvent effects, and molecular symmetry – all of which affect ISC and competing decay pathways.[9,14,16,18,19] For instance, electronic coupling induced by electron-withdrawing groups in DHPP is highly sensitive to positional isomerism (*e.g.*, 4-NO$_2$ and 3-NO$_2$) and to the presence of aryl spacers between D–A subunits,

a Institute of Organic Chemistry, Polish Academy of Sciences, Kasprzaka 44-52, 01-224 Warsaw, Poland. E-mail: dtgryko@icho.edu.pl

b Institute of Physics, Polish Academy of Sciences, Al. Lotników 32/46, 02-668 Warsaw, Poland. E-mail: crissetubal@ifpan.edu.pl

2344 | *Phys. Chem. Chem. Phys.*, 2026, **28**, 2344–2352

This journal is © the Owner Societies 2026

whose fine tuning can enhance the fluorescence of nitro-TAPPs.[8,20–22] Because these compounds are susceptible to ES-SB, their deactivation channel strongly depends on solvent polarity/proticity.[6–8,23] Interestingly, the inverse correlation between fluorescence quantum yields and the *N*-aryl torsion angle in bis-nitro-DHPPs arises from the increased charge separated state, which quenches their fluorescence.[8] In addition, structural distortion controls the ISC/IC non-radiative decay interplay, with planar geometries promoting IC through the suppression of S_1–T_1 spin–orbit coupling (SOC).[9]

In the broad portfolio of structural effects affecting the photophysics of these dyes, one aspect has so far been neglected, *i.e.* the influence of the electronic character of the substituent linked to the DHPP core through the pyrrolic nitrogen atom. Scattered observations have revealed that, for example, the presence of an *N*-4-nitrophenyl substituent causes quenching of emission as well as a strong bathochromic shift in absorption.[2] However, these random findings lack any systematic effect in the structure, which hampers the analysis of data. The goal of this paper is to design, synthesize and study the systematic series of TAPPs possessing various substituents at positions 1, 2, 4, and 5 and to attempt to elucidate the effect of these structural changes on absorption and emission. More specifically, we would like to investigate the influence of *N*-aryl substituents on the photophysics of TAPPs.

Design and synthesis

To rationalize the influence of different motifs showing distinct polarized effects at positions 1 and 4, we designed two sets of TAPPs varied at positions 2 and 5 (Fig. 1). In both sets, the *N*-aryl substituents are the same, and they provide a wide range of

1 R = 4-O_2N **2** R = 4-CN **3** R = 3-O_2N
4 R = 3-CN **5** R = 4-CH_3O **6** R = 4-*t*-Bu

7 R = 4-O_2N **8** R = 4-CN **9** R = 3-O_2N
10 R = 3-CN **11** R = 4-CH_3O **12** R = 4-*t*-Bu

Fig. 1 Structures of polarized TAPPs **1–12**.

electronic effects influencing the DHPP core, *i.e.* 4-nitrophenyl, 3-nitrophenyl, 4-cyanophenyl, 3-cyanophenyl, 4-methoxyphenyl and 4-*tert*-butylphenyl. Compounds **1–6** and **7–12** differ in the electronic character of substituents at positions 2 and 5. Dyes **1–6** bear 4-($CO_2C_6H_{13}$)C_6H_4 substituents as the electron-acceptors forming a clear quadrupolar A–D–A architecture, while in the second series (dyes **7–12**), 2,5-substituents possess the electron-neutral character. These substituents possess however the ester group electronically separated from the benzene ring, in order to secure suitable solubility in a broad range of solvents. All the products are easily accessible by the multi-component reaction between an aromatic amine, an aromatic aldehyde and butanedione, discovered in our group, giving the desired TAPPs in 5–41% yields.[2,24] Long alkyl chains attached to the aldehyde substrates are necessary to ensure sufficient solubility of the final products in organic solvents and can be easily introduced by carboxylate alkylation. This approach, so far unprecedented in the field of TAPPs,[25] allows adjusting the solubility by using alkyl halides of various lengths.

Photophysical properties

We measured the absorption and emission spectra and fluorescence quantum yields for dyes **1–12** in several solvents with a wide range of polarity to further examine this effect (Table 1, Fig. 2–4). What first catches the eye is that generally, electron-withdrawing groups in positions 1 and 4 shift the main absorption band hypsochromically, while, as we have shown previously, analogous substituents at positions 2 and 5 have the opposite effect.[2,8]

Absorption maxima of the main band of TAPP **1** in all the solvents are shifted by the presence of the nitro group outside the visible region, whereas λ_{abs} of **2–6** is above 380 nm in most of the cases (Fig. 2). At the same time for TAPPs **1** and **7**, there is a weak absorption shoulder in the range of 500–600 nm. Its characteristic features, *i.e.* broadness and very low intensity, prompted us to tentatively assign it to charge-transfer (CT) character.[26–28] This charge-transfer band is partly responsible for the visible yellow color of the solutions of these dyes. Weaker effect of that type is also observed in the case of TAPPs **2** and **8** possessing 4-CNC_6H_4 substituents. In the case of dye **8**, while λ_{abs} is hypsochromically shifted as far as 316–323 nm, depending on the solvent, an additional intriguing feature is a strong shoulder at approx. 370 nm (Fig. 3). Shifting the NO_2 group from position 4 to position 3 (TAPPs **3** and **9** *versus* TAPPs **1** and **7**) causes a small bathochromic shift of main λ_{abs} (Fig. 2 and Table 1).

The variation of spectral properties is broader in the case of TAPPs **7–12** than of **1–6**, where the electron-withdrawing ester groups linked with the DHPP core through biaryl linkages at positions 2 and 5 dominate the photophysics by creating a strong quadrupolar A–D–A system with the DHPP. Emission of dyes **1–4**, as compared to **5** and **6**, is shifted hypsochromically by the *N*-electron-withdrawing groups, while in the case of the second series, there is a large bathochromic shift into deep green in the fluorescence of **8** and **10** (compared to TAPPs **11**
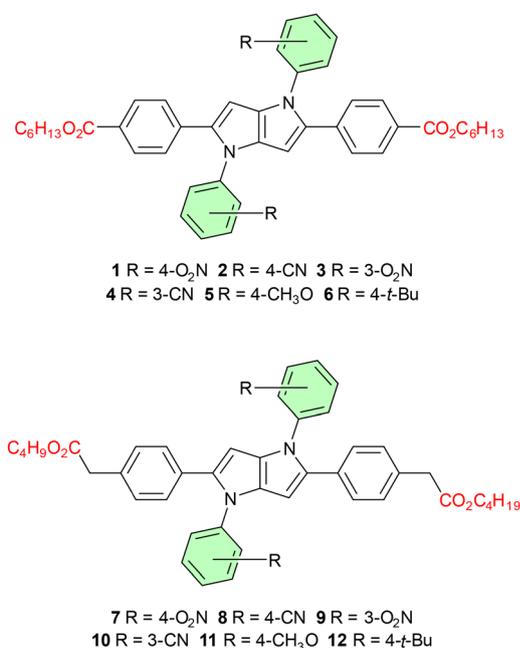
This journal is © the Owner Societies 2026

Phys. Chem. Chem. Phys., 2026, **28**, 2344–2352 | **2345**

Table 1 Photophysical properties of TAPPs **1–12** in a range of solvents

TAPP	Solvent	λ_{abs}/nm	$\varepsilon \times 10^3$ (cm^{-1} M^{-1})	λ_{em}/nm	$\Delta \bar{\nu}$ (cm^{-1})	Φ_f
1	Hexane	353	—	514	8900	0.031
	Toluene	364	57.8	450, 640	5300	0.0017
	Propyl butyrate	363	49.9	428, 700	4200	0.0005
	THF	367	62.9	—	—	0.00017
	CH$_2$Cl$_2$	368	68.1	461	5500	0.00011
	Acetonitrile	365	14.1	434, 550	4400	0.00003
	DMF	373	61.6	—	—	—
	DMSO	376	20.4	489	6100	0.00012
2	Hexane	—	—	—	—	—
	Toluene	393	24.6	447	3100	0.77
	Propyl butyrate	391	—	448	3300	0.79
	THF	394	—	454	3400	0.83
	CH$_2$Cl$_2$	393	—	455	3500	0.85
	Acetonitrile	389	—	469	4400	0.41
	DMF	398	—	473	4000	0.84
	DMSO	400	—	478	4100	0.77
3	Hexane	376	—	552	8500	0.004
	Toluene	386	45.6	450, 700	3700	0.00012
	Propyl butyrate	386	—	448, 780	3600	0.0002
	THF	388	—	450	3600	0.00012
	CH$_2$Cl$_2$	387	—	445	3400	0.00019
	Acetonitrile	385	—	445	3500	0.00003
	DMF	393	—	—	—	—
	DMSO	395	—	—	—	—
4	Hexane	380	—	428	3000	0.61
	Toluene	391	43.3	445	3100	0.78
	Propyl butyrate	389	—	447	3300	0.74
	THF	392	—	453	3400	0.8
	CH$_2$Cl$_2$	392	—	453	3400	0.8
	Acetonitrile	389	—	470	4400	0.5
	DMF	398	—	472	3900	0.75
	DMSO	400	—	479	4100	0.73
5	Hexane	396		438	2400	0.72
	Toluene	404	51.8	456	2800	0.82
	Propyl butyrate	402	—	456	2900	0.77
	THF	404	—	462	3100	0.79
	CH$_2$Cl$_2$	404	—	473	3600	0.85
	Acetonitrile	399	—	483	4400	0.74
	DMF	406	—	484	4000	0.84
	DMSO	408	—	492	4200	0.84
6	Hexane	394	—	438	2500	0.61
	Toluene	404	53.0	455	2800	0.77
	Propyl butyrate	400	—	455	3000	0.77
	THF	403	—	460	3100	0.75
	CH$_2$Cl$_2$	403	—	472	3600	0.81
	Acetonitrile	397	—	481	4400	0.7
	DMF	404	—	482	4000	0.81
	DMSO	406	—	491	4300	0.83
7	Hexane	341	—	573	12 000	0.0075
	Toluene	344	52.0	380, 720	2800	0.0003
	Propyl butyrate	342	—	403	4400	0.0001
	THF	343	—	—	—	0.000001
	CH$_2$Cl$_2$	342	47.2	606	13 000	0.00007
	Acetonitrile	339	56.9	382	3300	0.000005
	DMF	343	—	407	4600	0.0001
	DMSO	344	53.3	—	—	—
8	Hexane	316	—	426	8200	0.4
	Toluene	321	54.9	455	9200	0.24
	Propyl butyrate	319	—	485	11 000	0.082
	THF	320	—	509	12 000	0.044
	CH$_2$Cl$_2$	321	—	538	13 000	0.042
	Acetonitrile	318	—	581	14 000	0.0075
	DMF	321	—	571	14 000	0.013
	DMSO	323	—	586	14 000	0.007
9	Hexane	345	—	—	—	—
	Toluene	351	36.7	—	—	—
	Propyl butyrate	349	—	—	—	—
	THF	349	—	—	—	—
	CH$_2$Cl$_2$	350	—	—	—	—
	Acetonitrile	346	—	—	—	—

2346 | *Phys. Chem. Chem. Phys.*, 2026, **28**, 2344–2352

This journal is © the Owner Societies 2026

Table 1   (continued)

TAPP	Solvent	λ_{abs}/nm	$\varepsilon \times 10^3$ (cm^{-1} M^{-1})	λ_{em}/nm	$\Delta \bar{\nu}$ (cm^{-1})	Φ_f
	DMF	352	—	—	—	—
	DMSO	352	—	—	—	—
10	Hexane	347	—	425	5300	0.16
	Toluene	352	30.6	480	7600	0.043
	Propyl butyrate	348	—	509	9100	0.02
	THF	352	—	535	9700	0.012
	CH$_2$Cl$_2$	350	—	551	10 000	0.0096
	Acetonitrile	348	—	590	12 000	0.0019
	DMF	351	—	594	12 000	0.0031
	DMSO	354	—	605	12 000	0.0019
11	Hexane	355	—	403	3400	0.63
	Toluene	359	45.5	410	3500	0.65
	Propyl butyrate	356	—	407	3500	0.67
	THF	357	—	409	3600	0.69
	CH$_2$Cl$_2$	356	—	413	3900	0.63
	Acetonitrile	351	—	411	4200	0.68
	DMF	356	—	414	3900	0.72
	DMSO	356	—	417	4100	0.75
12	Hexane	355	—	405	3500	0.6
	Toluene	359	42.0	412	3600	0.65
	Propyl butyrate	356	—	409	3600	0.63
	THF	358	—	411	3600	0.63
	CH$_2$Cl$_2$	357	—	415	3900	0.61
	Acetonitrile	352	—	414	4300	0.64
	DMF	356	—	416	4100	0.67
	DMSO	358	—	418	4000	0.72

Quinine sulphate as a standard.

and **12**), as only in the presence of the cyano groups push–pull systems are created, however the fluorescence quantum yield (Φ_f) of this emission is low (Fig. 4 and Table 1).

Nitro groups almost entirely quench the fluorescence of the studied compounds, even in non-polar solvents, which is also different from what is observed for TAPPs possessing 4-nitrophenyl substituents at positions 2 and 5, which can have nearly quantitative emission in hexane.[8] Compound **9** does not show detectable fluorescence in any solvent. The emission of DHPPs **1**, **3** and **7** is also unmeasurable in some polar solvents, while in the others it is only slightly higher than the noise level (Fig. 3).

McRae plots were computed, and the results can be seen in Fig. S4 and Table S6. The data suggest that the most polarized

molecules are those containing nitrophenyl and cyanophenyl substituents.

The very low fluorescence quantum yields of some compounds point to the existence of an efficient radiationless channel of electronic relaxation. Among the weakly emissive molecular structures, most possess the nitro group (**1**, **3**, **7** and **9**) and two CN substituents (**8** and **10**). This may suggest that nitro groups introduce a low-lying singlet state of n$\pi^\star$ character that enhances the intersystem crossing process, as was discussed already in the Introduction. To investigate this supposition, emission spectra have been recorded at low temperature (77 K). Comparison of fluorescence spectra recorded at room temperature and 77 K is presented in Fig. S99. The overlap of
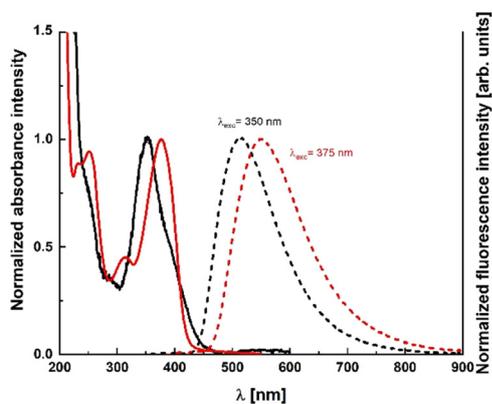

Fig. 2   Absorption (solid line) and emission (dotted line) of dyes **1** (black) and **3** (red) in *n*-hexane.
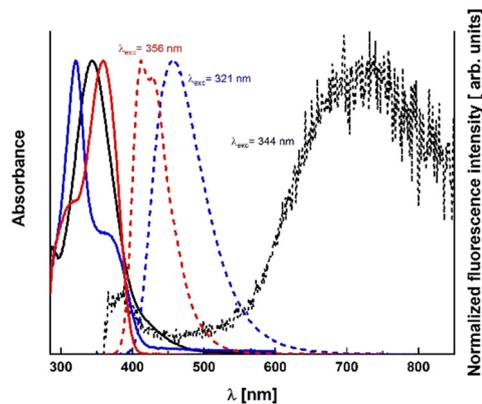

Fig. 3   Absorption (solid line) and emission (dotted line) of dyes **7** (black), **8** (blue) and **12** (red) in toluene.

This journal is © the Owner Societies 2026

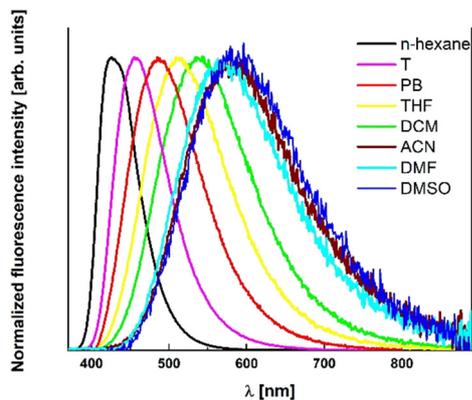*Phys. Chem. Chem. Phys.*, 2026, **28**, 2344–2352 | **2347**

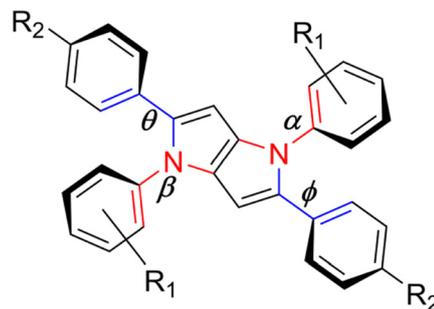Fig. 4 Solvatofluorochromism of TAPP **8** in various solvents.

the RT absorption spectrum with the 77 K fluorescence excitation spectrum proves that emission originates from monomers and not from aggregates. The most striking difference between the RT and 77 K emission spectra is the huge increase in fluorescence intensity, of the 100–1000 order. Lack of any structured phosphorescence spectrum is another observation. Thus, we conclude that in frozen solvent internal conversion is stopped (most likely due to restriction of twists/torsions) and the ISC process is not very efficient. The same conclusion holds for dyes **1**, **3** and **7** bearing NO_2 groups as well as for dye **10** possessing CN groups. This points to internal conversion as the very efficient channel of electronic relaxation that effectively quenches fluorescence at elevated temperatures.

Computational studies

In order to gain in-depth insight into the factors governing the fate of TAPP molecules in the excited state, we performed theoretical exploration at the *ab initio* level of theory. Most studies in the literature on DHPPs use density functional theory (DFT), typically using exchange–correlation functionals such as M06-2X,[10–14,29] B3LYP[8,15] and CAM-B3LYP.[8] However, wavefunction-based methods like ADC(2) outperform DFT because they avoid functional bias and provide a more accurate description of CT states.[16,29–32] In this work, computations were performed for all selected molecules in both fully relaxed and constrained to C_i point group conformations using structures with truncated alkyl chains.

This symmetry was imposed to prevent overestimating π-stacking between aromatic groups of TAPP branches, which may arise from the inherent limitations of MP2/ADC(2) in modelling dispersion forces.[33,34] Within the C_i framework, it is possible to optimize molecular structures of populated intramolecular charge transfer (ICT) excited states a_g (dark) and a_u (bright) separately, enabling the estimation of barriers to non-radiative decays of these systems. Ground state (S_0) structures optimized at the MP2/cc-pVDZ level of theory (without symmetry constraints) correspond to near-centrosymmetric geometries. Computed dihedral angles between the core and subunits range from 35 to 55° (Table 2). Remarkably, S_0 geometries remain

Table 2 Dihedral angles between the aryl substituents of the 1,4-dihydropyrrolo[3,2-*b*]pyrrole moiety for S_0 and $S_1(a_u)$ molecular structures corresponding to C_1 and C_i point groups, obtained at the MP2/ADC(2)/cc-pVDZ level of theory. Labels α, β, θ and φ are provided in the structure below

| TAPP | S_0 | | | | $S_1(a_u)$ | | | |
| | C_1 | | C_i | | C_1 | | C_i | |
	θ(φ)	α(β)	θ = φ	α = β	θ(φ)	α(β)	θ = φ	α = β
1	37	47	38	49	35(24)	87(55)	23(29)[a]	48(66)[a]
2	38	49	44	59	34(25)	91(55)	22	49
3	38	47	38	47	23(23)	46(46)	23	45
4	38	50	37	49	23(22)	50	22	50
5	35	53	36	54	26	56	24	57
6	36	53	36	52	24	55	24	55
7	48	55	40	48	34(22)	55(88)	28	52
8	40	48	40	48	45(34)	101(55)	36	45
9	39(46)	44	40	46	35(29)	64(53)	29	53
10	39	48	40	48	33(21)	59(55)	21	47
11	39	50	39	52	23(22)	53	20	52
12	37	52	38	51	20	52	20	52

[a] Dihedral angles computed for the a_g optimized structure.

non-polarized even with strong electron-accepting substituents, consistent with previous observations.[20]

Three vertical excited states were computed at the ADC(2)/cc-pVDZ level of theory for the MP2 ground state equilibrium structures of **1–12** (Table S1a) without symmetry constraints. The bright Franck–Condon (FC) state shows evenly distributed electronic density across TAPPs subunits, followed by higher-energy dark states.[7,20] Natural transition orbitals (Table S1b) analysis suggests that low-lying states correspond to ICT for dyes **1–3** and **7–10**, and to locally excited (LE) in the case of TAPPs **4–6**, **11** and **12**. The weak solvatochromism in **7–12** reflects suppressed D–A, whereas dyes **1–6** exhibit pronounced bathochromic shifts from direct ester-DHPP conjugation.[35]

To further characterize these FC states, excitation energies were also computed imposing C_i symmetry for the most representative systems, *i.e.* DHPPs **7** and **12** (Table S3). In both these cases, the a_g/a_u mixing is forbidden, preventing stabilization of the a_u bright state that would otherwise occur upon symmetry breaking. Compound **7** exhibits ICT with small overlap molecular orbitals of $^{FC}S_1$ (Fig. 5), resulting in low oscillator strength. Vertical excitation of compound **12** leads to intense LE emission, with frontier molecular orbitals localized on the DHPP core. Thus, the ratio of populating LE/ICT in non-polar solvents from $^{FC}S_1$ in **1–12** is modulated by the electron-accepting strength of 1,4-substituents.
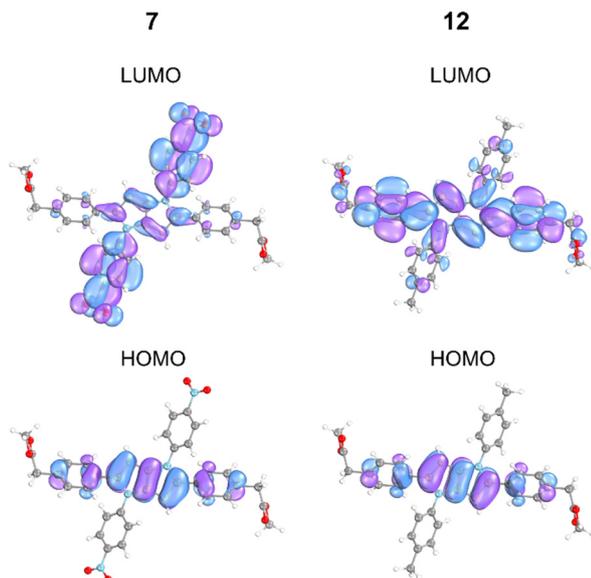
7   **12**

Fig. 5 Frontier molecular orbitals for selected compounds **7** and **12** obtained at the ADC(2)/cc-pVDZ level of theory for molecules computed with C_i symmetry.

While S_0 structures maintain near-C_i symmetry across all TAPPs, the S_1 minima are susceptible to ES-SB in dyes with strong *N*-electron-accepting groups (*e.g.*, 4-NO$_2$ and 4-CN substituents).[5,7,20] The symmetry breaking induced upon photoexcitation promotes stabilization of charge-separated twisted intramolecular charge transfer (TICT), evidenced by a $\approx 40°$ increase in *N*-aryl dihedral angles in the S_1 optimized structures for unconstrained conformation (C_1 point group) with respect to structures computed imposing C_i symmetry (Table 2). The weak inter-branch dispersion forces that promote the formation of transient dipoles in compounds **1–3**, and **7–10** (Table S4) stabilize dark TICT states, which, with the exception of **2** and **8**, effectively quench their fluorescence, are consistent with experimental observations. Conversely, this behavior is not observed for TAPPs with dominant LE character (**4–6** and **11**, **12**).

Examining Scheme S1 revealed that the strong A–D–A electronic coupling in **1–6** decreases electron density rearrangement upon excitation, promoting the population of a LE state, leading to larger fluorescence quantum yields compared to dyes **7–12**. Overall, regarding DHPPs **1–6**, the *N*-substituent's electron-donating/accepting strength controls their main deactivation channel, either *via* ES-SB or LE emission.

Upon photoexcitation in centrosymmetric TAPPs corresponding to the C_i point group, the S_1^{FC} state relaxes into two ICT states with distinct symmetries: a bright a$_u$ state and a dark a$_g$ state, with the latter decaying non-radiatively to S_0. The energy barrier between these states controls the IC rate and consequently the fluorescence quantum yields (Table 1).[36] To estimate the a$_u$/a$_g$ population barrier, geometry optimizations were performed for both excited states for all molecules, and the results were summarized in the simplified Jablonski diagrams (Fig. 6). Compounds **1** and **7**, which possess small energy gaps between their a$_g$ and a$_u$ states, are expected to access the

conical intersection (CI) to the ground state in a barrierless fashion, efficiently quenching emission from the 1a$_u$. C_i symmetry constraints limit large amplitude movements between TAPP subunits. However, 1a$_g$ exhibits increased TICT state character compared to a$_u$, as suggested by an $18°$ increase in the twist along σ-bonds between the DHPP core and the 4-NO$_2$C$_6$H$_4$ substituents. Thus, the low fluorescence quantum yields observed for these compounds arise from their strong ICT character and symmetry breaking, which promotes seamless access to the S_1/S_0 conical intersection.[8,27] This conclusion corresponds well with results by Vullev and co-workers who noticed that in TAPPs strengthening D–A electronic coupling decreases CT and propensity for ES-SB.[20]

Conversely, **6** and **12** exhibit a significant barrier for IC (*i.e.* the a$_u$ → a$_g$) (≈ 0.6 eV), promoting strong emission from the a$_u$ state. Thus, the barrier height governs the emission efficiency of TAPPs in non-polar solvents such as hexane, with fluorescence quantum yields equal to 0.031, 0.61, 0.0003, and 0.65 for **1**, **6**, **7**, and **12**, respectively. However, while this approach can reasonably correlate the measured fluorescence intensity with the height of the a$_u$/a$_g$ barrier, in both series, there are a few notable exceptions: compound **2** displays intense fluorescence while **3** and **10** are barely fluorescent, despite exhibiting small and large barriers for IC, respectively. The strong fluorescence observed for compound **2** is attributed to weaker electronic coupling between the *N*-4-cyanophenyl group and the DHPP core, in contrast to compound **1**, which promotes the population of the LE excited state (Fig. S3) and enhances its emission. In contrast, compounds **3** and **10** exhibit weak fluorescence despite a predicted high barrier for accessing their non-emissive a$_g$ state. Unlike *para*-NO$_2$,[8,20] the *meta*-NO$_2$ group disrupts conjugation between DHPP and nitroaryl groups, resulting in an asymmetric electronic distribution which makes these dyes susceptible to ES-SB, promoting the population of a non-emissive species, particularly in polar solvents.[6,13,18,20,37]

Nitro groups bonded to DHPPs act as pseudo-heavy atoms and enhance spin–orbit coupling (SOC), modulating the ISC/IC branching ratio in non-radiative deactivation pathways, as observed in 2,5-nitro-pyrrolo[3,2-*b*]pyrroles.[8] In contrast, as can be seen in Fig. 4, no significant triplet-mediated deactivation is predicted due to the large singlet–triplet energy gap ($\Delta E_{ST} \approx 1$ eV). Thus, despite having nitroaryl groups, IC remains the main dissipation channel for the **1**, **3**, **7** and **9** gap ($\Delta E_{ST} \approx 1$ eV).

Solvation effects were evaluated using the COSMO continuum approximation (DMSO was chosen as the solvent) to compute excitation/emission energies. Computed FC states for selected compounds **1**, **3**, and **8** suggest minimal solvatochromism (approximately 0.1 eV between vacuum and solution), consistent with the small redshift observed in their absorption bands (Table 1). Emission bands for compounds **1**, **3**, **7**, **8** and **10** were too weak to estimate their solvatochromism.

Interestingly, despite both having 4-CN substituents, compounds **2** and **8** exhibit markedly distinct emission profiles. The quadrupolar A–D–A architecture present in **2** favors strong LE emission, as also observed for dyes **4**, **5**, **6**, **11** and **12**, which

This journal is © the Owner Societies 2026

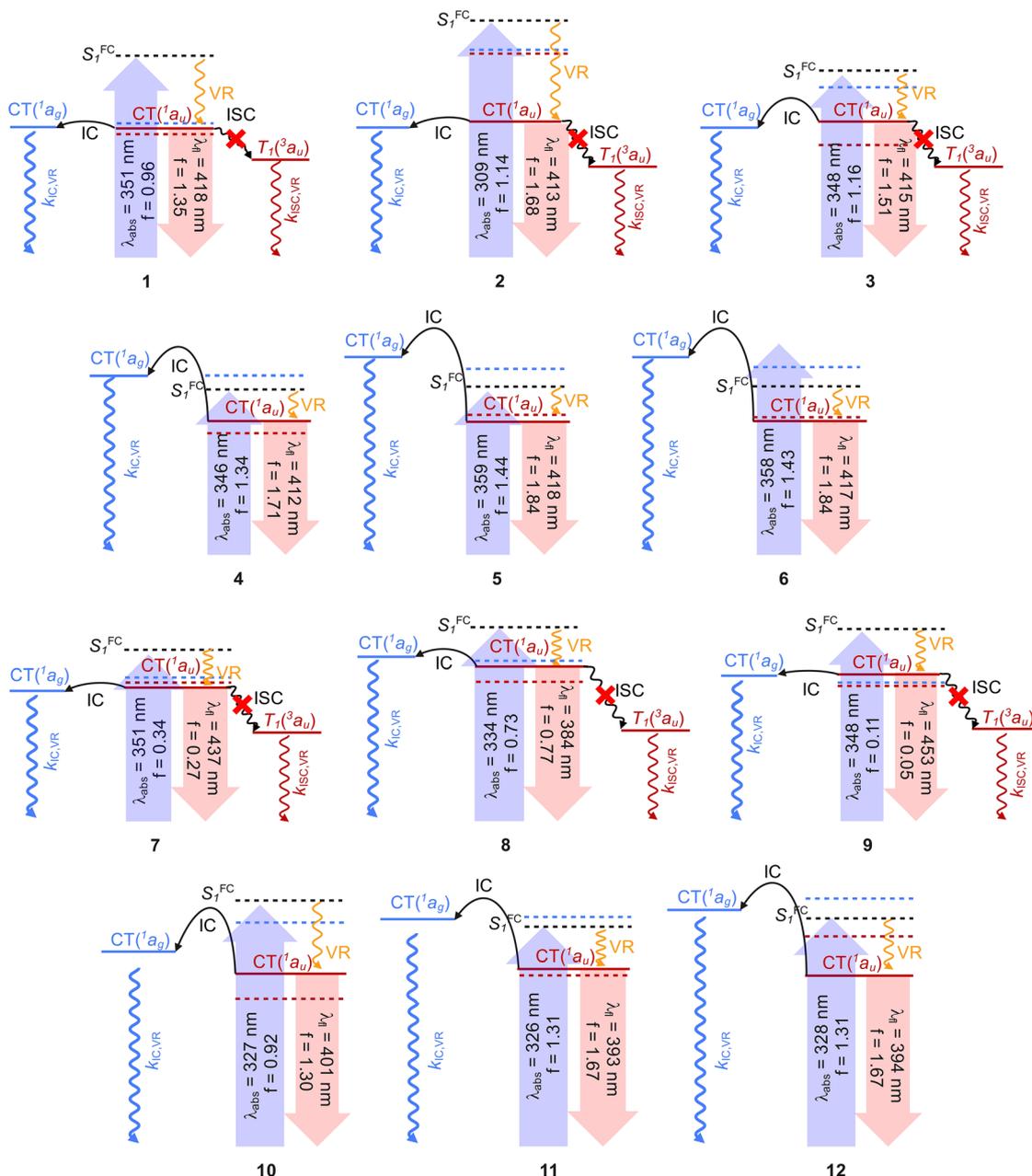*Phys. Chem. Chem. Phys.*, 2026, **28**, 2344–2352 | **2349**

Fig. 6 Jablonski diagrams for dyes **1–12** computed at the ADC(2)/cc-pVDZ level of theory. Solid horizontal lines represent the adiabatic energies of a_g and a_u states. Dashed lines represent vertical energies computed for S_1^{FC}, a_u and a_g (marked in black, red and blue, respectively). Wavy straight arrows represent internal conversion (IC), intersystem crossing (ISC), and vibrational relaxation (VR), while straight arrows show fluorescence, respectively. Barriers for the population of a_g are represented as black curves.

is redshifted by 0.1–0.3 eV with increasing solvent polarity. On the other hand, the disruption of D–A electronic coupling by the addition of a CH_2 spacer promotes ICT for **8**, effectively suppressing its fluorescence, particularly in polar solvents.[10,18] The absence of fluorescence in **9**, regardless of solvent polarity, is associated with the disruption of the conjugation between DHPP and 3-nitrophenyl moieties, which promotes the near degeneracy between the π-system and the nitrogen lone-pair orbitals. As a result, this compound is susceptible to strong vibronic mixing (pseudo-Jahn–Teller effect), resulting in the

population of a non-emissive chiral hybrid S_1 state, as can be seen in Fig. S3.

This study extends beyond excited-state symmetry breaking, which was investigated for DHPPs.[6,7,35] The influence of substituents linked to the DHPP core *via* a nitrogen atom has a remarkably different character compared to the influence of C2- and C3-substituents. The strong influence of electron-withdrawing substituents at positions 1 and 4 is reduced if electron-withdrawing substituents are present at positions 2 and 5. The disruption of the electronic coupling increases

2350 | *Phys. Chem. Chem. Phys.*, 2026, **28**, 2344–2352

This journal is © the Owner Societies 2026

charge separation between subunits. This effect is particularly strong for *N*-4-nitrophenyl substituents, which are more susceptible to the formation of transient dipole moments and the population of dark states, effectively suppressing their fluorescence. This effect is amplified in polar solvents, which further stabilizes charge-separated states. While the height of the dark/bright state barriers has a direct correlation with the measured quantum yields, there are a few exceptions. The most interesting case is TAPP **9**, for which no fluorescence is observed, regardless of the solvent polarity. Based on our computations, the nπ*–ππ* near degeneracy would make this molecule susceptible to strong vibronic mixing, quenching its emission. It is worth noting that intersystem crossing is not operating efficiently for *N*-4-nitrophenyl derivatives, as indicated by the absence of phosphorescence observed at cryogenic temperatures. Thus, internal conversion drives the radiationless deactivation of both series of compounds.

The above-described results will play a vital role in the design of TAPPs in the future. The current results clearly point out that the 4-methoxyphenyl substituent does not interfere markedly with strongly emissive characteristics of tetraarylpyrrolo[3,2-*b*]pyrroles possessing either electron-withdrawing substituents or neutral substituents at positions 2 and 5. This is of paramount importance since this type of dye is often investigated and substituting methyl with a longer and branched alkyl chain can enable the increase of the solubility. The latter one is critical since tetraarylpyrrolo[3,2-*b*]pyrroles are notoriously poorly soluble. At the same time, TAPPs bearing the 4-cyanophenyl or 3-cyanophenyl substituents at positions 1 and 4 have a strong fluorescence only of electron-withdrawing groups present at positions 2 and 5. This is a critical observation since especially 4-cyanophenyl groups help to regulate the photostability of TAPPs.

Conclusions

The comprehensive study of photophysical properties of 1,4-dihydropyrrolo[3,2-*b*]pyrroles enabled us to draw the following conclusions. (1) If electron-withdrawing 4-(CO$_2$R)C$_6$H$_4$ substituents are present at positions 2 and 5, they dominate the photophysics of these DHPPs (fluorescence is strong across the scale of solvents' polarity), unless nitrophenyl substituents are present at position 1 and 4. (2) If 4-nitrophenyl substituents are located at positions 1 and 4, non-radiative decay is dominated by the population of a TICT excited state (a$_g$), which is predicted to occur seamlessly from the bright state a$_u$. (3) If, however, the substituents at positions 2 and 5 are electron-neutral and *N*-substituents are electron-withdrawing, strong quenching of fluorescence is observed in polar solvents. We attribute this behavior to ES-SB and the formation of transient dipole moments. This, in turn, leads to the stabilization of charge-separated states and favoring of non-radiative decay pathways. This study provides a foundation for the design of DHPP with fine-tuned, tailored photophysical properties.

Author contributions

Conceptualization: D. T. G. and W. D. P.; investigation: W. D. P., Z. K., C. A. B., O. M. and M. B.; supervision: D. T. G.; visualization: W. D. P., C. A. B., and M. B.; writing – original draft: W. D. P., D. T. G., C. A. B., O. M. and M. B.; writing – review and editing: W. D. P., D. T. G., and C. A. B. All the authors discussed the results and commented on the manuscript.

Conflicts of interest

There are no conflicts to declare.

Data availability

The data supporting this article have been included as part of the supplementary information (SI). Supplementary information: detailed synthetic protocols, characterization data; ^{1}H, ^{13}C{^{1}H} NMR and HRMS spectra, computational details (including Cartesian coordinates), photophysical measurement and additional figures as mentioned in the text. See DOI: https://doi.org/10.1039/d5cp03474d.

Acknowledgements

Notes and references

1 H. Hemetsberger and D. Knittel, *Monatsh. Chem.*, 1972, **103**, 194–204.
2 A. Janiga, E. Glodkowska-Mrowka, T. Stoklosa and D. T. Gryko, *Asian J. Org. Chem.*, 2013, **2**, 411–415.
3 M. Krzeszewski, O. Vakuliuk, M. Tasior, A. Wołos, R. Roszak, K. Molga, M. B. Teimouri, B. A. Grzybowski and D. T. Gryko, *J. Am. Chem. Soc.*, 2025, **147**, 15636–15644.
4 M. Krzeszewski, Ł. Dobrzycki, A. L. Sobolewski, M. K. Cyrański and D. T. Gryko, *Chem. Sci.*, 2023, **14**, 2353–2360.
5 G. Sanil, M. Krzeszewski, W. Chaładaj, W. Danikiewicz, I. Knysh, Ł. Dobrzycki, O. Staszewska-Krajewska, M. K. Cyrański, D. Jacquemin and D. T. Gryko, *Angew. Chem., Int. Ed.*, 2023, **62**, e202311123.

This journal is © the Owner Societies 2026

Phys. Chem. Chem. Phys., 2026, **28**, 2344–2352 | **2351**

6 B. Dereka, A. Rosspeintner, M. Krzeszewski, D. T. Gryko and E. Vauthey, *Angew. Chem., Int. Ed.*, 2016, **55**, 15624–15628.

7 C. Govind, E. Balanikas, G. Sanil, D. T. Gryko and E. Vauthey, *Chem. Sci.*, 2024, **15**, 17362–17371.

8 Y. M. Poronik, G. V. Baryshnikov, I. Deperasińska, E. M. Espinoza, J. A. Clark, H. Ågren, D. T. Gryko and V. I. Vullev, *Commun. Chem.*, 2020, **3**, 190.

9 K. Górski, D. Kusy, S. Ozaki, M. Banasiewicz, R. Valiev, S. R. Sahoo, K. Kamada, G. Baryshnikov and D. T. Gryko, *J. Mater. Chem. C*, 2024, **12**, 1980–1987.

10 M. Banasiewicz, R. Stężycki, G. D. Kumar, M. Krzeszewski, M. Tasior, B. Koszarna, A. Janiga, O. Vakuliuk, B. Sadowski, D. T. Gryko and D. Jacquemin, *Eur. J. Org. Chem.*, 2019, 5247–5253.

11 M. Tasior, G. Clermont, M. Blanchard-Desce, D. Jacquemin and D. T. Gryko, *Chem. – Eur. J.*, 2019, **25**, 598–608.

12 Y. M. Poronik, L. M. Mazur, M. Samoć, D. Jacquemin and D. T. Gryko, *J. Mater. Chem. C*, 2017, **5**, 2620–2628.

13 Ł. G. Łukasiewicz, M. Rammo, C. Stark, M. Krzeszewski, D. Jacquemin, A. Rebane and D. T. Gryko, *ChemPhotoChem*, 2020, **4**, 508–519.

14 R. Orłowski, M. Banasiewicz, G. Clermont, F. Castet, R. Nazir, M. Blanchard-Desce and D. T. Gryko, *Phys. Chem. Chem. Phys.*, 2015, **17**, 23724–23731.

15 M. Krzeszewski, T. Kodama, E. M. Espinoza, V. I. Vullev, T. Kubo and D. T. Gryko, *Chem. – Eur. J.*, 2016, **22**, 16478–16488.

16 S. Hatanaka, T. Ono, Y. Yano, D. T. Gryko and Y. Hisaeda, *ChemPhotoChem*, 2020, **4**, 138–143.

17 B. Szymański, S. R. Sahoo, O. Vakuliuk, R. Valiev, R. Ramazanov, P. Łaski, K. N. Jarzembska, R. Kamiński, M. B. Teimouri, G. Baryshnikov and D. T. Gryko, *Chem. Sci.*, 2024, **16**, 2170–2179.

18 Ł. G. Łukasiewicz, H. G. Ryu, A. Mikhaylov, C. Azarias, M. Banasiewicz, B. Kozankiewicz, K. H. Ahn, D. Jacquemin, A. Rebane and D. T. Gryko, *Chem. – Asian J.*, 2017, **12**, 1736–1748.

19 D. H. Friese, A. Mikhaylov, M. Krzeszewski, Y. M. Poronik, A. Rebane, K. Ruud and D. T. Gryko, *Chem. – Eur. J.*, 2015, **21**, 18364–18374.

20 J. A. Clark, D. Kusy, O. Vakuliuk, M. Krzeszewski, K. J. Kochanowski, B. Koszarna, O. O'Mari, D. Jacquemin, D. T. Gryko and V. I. Vullev, *Chem. Sci.*, 2023, **14**, 13537–13550.

21 A. M. Hawks, D. Altman, R. Faddis, E. M. Wagner, K. J. J. Bell, A. Charland-Martin and G. S. Collier, *J. Phys. Chem. B*, 2023, **127**, 7352–7360.

22 A. M. Hawks, L. M. Daniel, V. S. Sorto, J. Mauro, P. Skiouris and G. S. Collier, *ACS Appl. Opt. Mater.*, 2024, **2**, 1235–1244.

23 F. Terenziani, A. Painelli, C. Katan, M. Charlot and M. Blanchard-Desce, *J. Am. Chem. Soc.*, 2006, **128**, 15742–15755.

24 M. Tasior, O. Vakuliuk, D. Koga, B. Koszarna, K. Górski, M. Grzybowski, Ł. Kielesiński, M. Krzeszewski and D. T. Gryko, *J. Org. Chem.*, 2020, **85**, 13529–13543.

25 G. Sanil, B. Koszarna, Y. M. Poronik, O. Vakuliuk, B. Szymański, D. Kusy and D. T. Gryko, *Adv. Heterocycl. Chem.*, 2022, **138**, 335–409.

26 J. B. Derr, J. Tamayo, J. A. Clark, M. Morales, M. F. Mayther, E. M. Espinoza, K. Rybicka-Jasińska and V. I. Vullev, *Phys. Chem. Chem. Phys.*, 2020, **22**, 21583–21629.

27 A. Neubauer, J. Bendig and W. Rettig, *Chem. Phys.*, 2009, **358**, 235–244.

28 S. Lee, M. Jen, T. Jang, G. Lee and Y. Pang, *Sci. Rep.*, 2022, **12**, 1–11.

29 D. Mester and M. Kállay, *J. Chem. Theory Comput.*, 2022, **18**, 1646–1662.

30 C. R. Zhang, J. S. Sears, B. Yang, S. G. Aziz, V. Coropceanu and J. L. Brédas, *J. Chem. Theory Comput.*, 2014, **10**, 2379–2388.

31 Z. L. Cai, M. J. Crossley, J. R. Reimers, R. Kobayashi and R. D. Amos, *J. Phys. Chem. B*, 2006, **110**, 15624–15632.

32 A. Dreuw and M. Head-Gordon, *J. Am. Chem. Soc.*, 2004, **126**, 4007–4016.

33 N. M. P. Rosa and I. Borges, *J. Comput. Chem.*, 2024, **45**, 2885–2898.

34 M. O. Sinnokrot and C. D. Sherrill, *J. Phys. Chem. A*, 2006, **110**, 10656–10668.

35 A. H. Balawi, S. Stappert, J. Gorenflot, C. Li, K. Müllen, D. Andrienko and F. Laquai, *J. Phys. Chem. C*, 2019, **123**, 16602–16613.

36 G. W. Robinson and R. P. Frosch, *J. Chem. Phys.*, 1963, **38**, 1187–1203.

37 B. Dereka, A. Rosspeintner, R. Stężycki, C. Ruckebusch, D. T. Gryko and E. Vauthey, *J. Phys. Chem. Lett.*, 2017, **8**, 6029–6034.

2352 | *Phys. Chem. Chem. Phys.*, 2026, **28**, 2344–2352

This journal is © the Owner Societies 2026